International Journal of Biological Macromolecules 139 (2019) 1054–1062

Contents lists available at ScienceDirect

International Journal of Biological Macromolecules

journal homepage: http://www.elsevier.com/locate/ijbiomac

Biomimetic hybrid scaffold consisting of co-electrospun collagen and PLLCL for 3D cell culture

Esra Türker [a], Ümit Hakan Yildiz [b], Ahu Arslan Yildiz [a,*]

[a] Department of Bioengineering, Izmir Institute of Technology (IzTech), 35430 Izmir, Turkey
[b] Department of Chemistry, Izmir Institute of Technology (IzTech), 35430 Izmir, Turkey

ARTICLE INFO

Article history:
Received 2 July 2019
Received in revised form 8 August 2019
Accepted 8 August 2019
Available online 09 August 2019

Keywords:
Collagen
Biomimetic scaffold
Co-electrospinning
3D cell culture
Tissue engineering

ABSTRACT

Electrospun collagen is commonly used as a scaffold in tissue engineering applications since it mimics the content and morphology of native extracellular matrix (ECM) well. This report describes "toxic solvent free" fabrication of electrospun hybrid scaffold consisting of Collagen (Col) and Poly(L-lactide-*co*-ε-caprolactone) (PLLCL) for three-dimensional (3D) cell culture. Biomimetic hybrid scaffold was fabricated via co-spinning approach where simultaneous electrospinning of PLLCL and Collagen was mediated by polymer sacrificing agent Polyvinylpyrrolidone (PVP). Acidified aqueous solution of PVP was used to solubilize collagen without using toxic solvents for electrospinning, and then PVP was readily removed by rinsing in water. Mechanical characterizations, protein adsorption, as well as biodegradation analysis have been conducted to investigate feasibility of biomimetic hybrid scaffold for 3D cell culture applications. Electrospun biomimetic hybrid scaffold, which has 3D-network structure with 300–450 nm fiber diameters, was found to be maximizing cell adhesion through assisting NIH 3T3 mouse fibroblast cells. 3D cell culture studies confirmed that presence of collagen in biomimetic hybrid scaffold have created a major impact on cell proliferation compared to conventional 2D systems on long-term, also cell viability increased with the increasing amount of collagen.

1. Introduction

Traditional two-dimensional (2D) cell culture methods where cells are cultivated on flat surfaces are commonly used in biological applications [1–4]. However, 2D cell culture does not reflect the 3D physiology and function of real tissue. In native tissue, all cells are embedded in a complex three-dimensional (3D) fibrillar network; namely extracellular matrix (ECM) providing physical and biochemical signals to facilitate cellular activities [5]. ECM also ensures diversifying of tissues by the fact that coexisting of different cell types are embedded in 3D microenvironment with varied ECM components. Therefore, transition from conventional 2D monolayer cell culture model to more realistic and controllable 3D cell culture models is required for functional tissue formation [6].

Scaffold-based tissue engineering is commonly used approach to overcome restrictions of 2D cell culturing, where natural and synthetic polymers are used to mimic the physical structure and microenvironment of native tissues [7,8]. Among 3D scaffold fabrication techniques; such as salt-particle leaching [9–12], rapid prototyping [13–17], freeze drying [18–20] and gas foaming [21–23], electrospinning [24–28] is one of the most established and advanced manufacturing techniques that yields fiber-like and porous structure similar to natural ECM [29,30]. Interconnected porous fibers that range from nano- to micro-scale provide easy transport of nutrients and removal of metabolic waste, which is important for cell growth and tissue regeneration.

To date, varied synthetic polymers; including polylactic acid, polyglycolic acid, poly (ε-caprolactone), poly (L-lactide-co-ε-caprolactone), and natural biopolymers such as; collagen, elastin, hyaluronic acid, silk, fibrinogen, have been employed for electrospinning [24,31–36]. Collagen is the major component of ECM, which is commonly used in tissue engineering studies to mimic native microenvironment [37–40]. Collagen plays an important role in tissue engineering since it promotes cell proliferation and differentiation. Therefore, it has been highly utilized either as a scaffold material by itself, or as an additive due to its excellent biocompatibility, biodegradability and cell adhesion features. However, electrospinning of collagen is limited by solubility related processing problems owing to collagen's cross-linked triple helix structure. Generally, highly toxic organic solvents such as; hexafluoro isopropanol (HFIP) are used to solubilize collagen which mostly results in denaturation of collagen [31,41–46].

Therefore, we developed a new methodology where toxic solvent free process of the collagen can be accomplished with the help of aqueous polymer sacrificing agent; PVP. So far, to the best of our knowledge,

* Corresponding author.
E-mail address: ahuarslan@iyte.edu.tr (A. Arslan Yildiz).

https://doi.org/10.1016/j.ijbiomac.2019.08.082
0141-8130/

there have been no reports that combined polymer sacrificing agent usage with co-electrospinning. Here, co-electrospinning technique is associated with polymer sacrificing agent; where PVP works as a transporter material for easy spinning of collagen and then acts as a sacrificing agent for integration of collagen. Poly (L-lactide-*co*-ε-caprolactone) (PLLCL) is an elastic, biocompatible, and biodegradable synthetic polymer, which is approved by Food and Drug Administration (FDA) for human clinical applications [47–52]. Therefore, it is used as a base scaffold for collagen integration. Biomimetic PLLCL/PVP/Col hybrid scaffolds were fabricated by co-electrospinning methodology. Afterwards PVP was easily removed from hybrid electrospun scaffolds via solubilizing in water. Morphology, porosity, mechanical properties, chemical and biological content was investigated through SEM, FTIR, immunostaining, tensile strength, contact angle, protein adsorption and biodegradation analyses. For in-vitro assessment, NIH 3T3 mouse fibroblast cells were used as a model to investigate cellular biocompatibility, cell adhesion and proliferation on PLLCL/Col hybrid scaffolds. Cellular studies confirmed that the biomimetic scaffold composed of PLLCL and Collagen Type I mimics well the morphology and function of native ECM.

2. Experimental

2.1. Materials

Poly (L-Lactide-*co*-ε-caprolactone) (PLLCL) was purchased from Evonik Industries. Polyvinylpyrrolidone (PVP) (Mw 360.000), dimethylformamide (DMF), dichloromethane (DCM), acetic acid, collagen Type I from calf skin, lysozyme from chicken egg white in the form of lyophilized powder and bovine serum albumin as lyophilized powder (BSA) was purchased from Sigma Aldrich. Tween80, tween20, tritonX-100 and sodium dodecyl sulfate (SDS) was purchased from Bioshop. Anti-Collagen Type I-FTIC Antibody was purchased from Merck. For cell culture studies; NIH-3T3 mouse fibroblast cell line (ATCC® CRL-1658™), high glucose Dulbecco's modified eagle's medium (DMEM), penicillin-streptomycin (P/S), trypsin-EDTA solution (0.25%, sterile-filtered, BioReagent) from Sigma Aldrich and fetal bovine serum (FBS-Gibco), phosphate buffer saline (PBS, pH 7.4 10×, Gibco), dimethylsulphoxide (DMSO, Carlo Erba) were used. Resazurin sodium salt from ChemCruz and CytoCalcein AM and Propidium Iodide dye (AAT Bioquest) were used for cytotoxicity, proliferation and live/dead assays.

2.2. Fabrication of PLLCL/PVP/collagen hybrid scaffolds

Electrospun polymer scaffolds; pristine PLLCL and PLLCL/PVP/Col, were fabricated by using Inovenso (Ne300) electrospinning system. 10 wt% PLLCL was dissolved in (4.5:0.5) DCM:DMF and stirred overnight. PLLCL solution was electrospun through 20 mL syringe and 20 gauge blunt tip needle at a flow rate of 3.0 mL/h, voltage 25 kV, and tip collector distance 18 cm. Fibers were collected on aluminum foil coated collector. Collected fibers were dried at room temperature prior to further characterization steps and cell studies. For the fabrication of PLLCL/PVP/Col hybrid scaffolds, 10 wt% PLLCL was dissolved in (4.5:0.5) DCM: DMF, 15 wt% PVP was dissolved in deionized water and stirred overnight 1% collagen type I were solubilized in deionized water which was acidified with 0.1 M acetic acid. 1% collagen type I was mixed with 15 wt% PVP solution by continuous stirring. Hybrid polymer scaffolds were fabricated by co-electrospun process of PLLCL and PVP/Col. Co-electrospinning of PLLCL/PVP/Col was accomplished through following parameters; the flow rate of PLLCL was 3 mL/h and for PVP/1%Col was 2.5 mL/h, distance 10.5 cm and voltage was arranged to 30 kV. Further, collected PLLCL/PVP/Col scaffolds were immersed into deionized water for 2 days to solubilize and remove PVP. Hybrid scaffolds were dried at room temperature and stored at −20 °C for further analysis and cell studies.

2.3. Characterization of hybrid scaffolds

Surface morphology and fiber diameter of pristine PLLCL, PLLCL/PVP/Col and PLLCL/Col scaffolds (after removing PVP) were visualized via scanning electron microscope (SEM; FEI Quanta 250 FEG). Through argon gas, surface of the scaffolds was coated with thin gold layer (Emitech K550X). Image J Software (NIH) was used to evaluate average fiber diameters of scaffolds.

Fourier Transform Infrared (Perkin Elmer - diamond/ZnSe crystal) analysis was performed in ATR mode to identify the presence and absence of PVP and collagen in electrospun scaffolds. The optimum scan range was between 650 and 4000 cm^{-1} wavenumbers. The resolution rate was 4 cm^{-1} and scan number was 20. Obtained data was plotted and analyzed by OriginPro (Northampton, MA) software.

Wettability of hybrid scaffolds was investigated using water contact angle measurements. The contact angle of scaffolds; PLLCL, PLLCL/PVP/Col, and PLLCL/Col (after removing PVP) were measured by contact angle meter in static mode after dispensing 5 μL water onto scaffolds. Five different sets were measured for each individual scaffold and the average value was evaluated (Attension).

TA XT Plus Texture Analyzer (Stable Micro Systems) was used to analyze the mechanical strength of PLLCL, PLLCL/PVP, PLLCL/PVP/Col, and PLLCL/Col (after removing PVP) scaffolds. Four replications of each scaffold were tested while using 5 kg load, and elongation speed was adjusted to 20 mm/min. Stress-strain curves, young modulus and ultimate tensile strength were evaluated.

2.4. Collagen immunostaining

PLLCL, PLLCL/PVP, PLLCL/PVP/Col, and PLLCL/Col (after removing PVP) scaffolds were stained by Monoclonal IgG1 conjugated to FITC antibody against collagen to examine the presence of collagen after sacrificing agent removal. First, 1% BSA was used as blocking agent, and Monoclonal IgG1 conjugated to FITC antibody against collagen was mixed with 0.5% BSA, then scaffolds were incubated overnight at room temperature. After incubation, scaffolds were rinsed with 1× PBS three times. Fluorescence microscope (Zeiss Observer Z1) was used to visualize collagen containing electrospun scaffolds.

2.5. Protein adsorption analysis

Bicinchoninic acid (BCA) assay (Pierce™, Thermo Scientific) was used to determine total amount of adsorbed protein on scaffolds. PLLCL, PLLCL/PVP and PLLCL/PVP/Col scaffolds were screened against BSA solution in which protein concentration range was 25–2000 μg/mL. For each concentration three replications were made. SDS was used to solubilize adsorbed proteins on PLLCL scaffolds. Absorbance was measured at 562 nm (Fisher Scientific™ accuSkan™ GO UV/Vis Microplate Spectrophotometer) and graphs were plot by Origin Pro (Northampton, MA) software.

2.6. Biodegradation analysis

To analyze the biodegradation, PLLCL/Col scaffolds were incubated in enzymatic solutions. Scaffolds were cut in square shapes (1.5 cm^2 × 1.5 cm^2), and then scaffolds were immersed in 1.5 μg/mL of lysozyme containing 1× PBS solution. Scaffolds were incubated at 37 °C with constant shaking for 20 weeks (Thermo Shaker MS100). Prior to analysis, scaffolds were washed with deionized water and dried in vacuum desiccator. Biodegradation analysis was done for each scaffold through weight loss calculation and morphology change that was visualized by SEM.

2.7. 3D cell culture, cell viability and toxicity studies

NIH 3T3 mouse fibroblast cell line was used as a model system for 3D cell culture formation. Co-electrospun PLLCL/PVP/Col scaffolds were immersed in deionized water for 2 days to remove sacrificing agent PVP. PLLCL, PLLCL/PVP, PLLCL/PVP/Col and PLLCL/Col scaffolds were sterilized under ultraviolet light (UV) for 30 min and placed in 96 well plate (BioLite, Thermo Scientific) with three replications. 2D cultured and expanded NIH 3T3 cells were harvested by using 0.25% Trypsin/EDTA solution, and cells were seeded over each scaffold with a 3D control groups (PLLCL) and incubated overnight. Scaffolds were taken from culture medium and put in clear wells, washed with 1× PBS to remove unattached cells and completed with fresh culture medium.

Cytotoxicity, proliferation and viability analysis were performed up to 14 days by alamar blue and live/dead assays. Before each analysis, 3D cell cultured hybrid scaffolds were washed with 1× PBS. For alamar blue analysis 1% stock solution of resazurin sodium salt was prepared and diluted to be 0.01% as a final concentration in culture medium and incubated 2–4 h. After incubation, absorbance values of solutions were measured at 570–600 nm.

CytoCalcein™ Green and Propidium Iodide (PI) dyes (AATBioquest) were used for live/dead analysis of short and long-term 3D cell cultures.

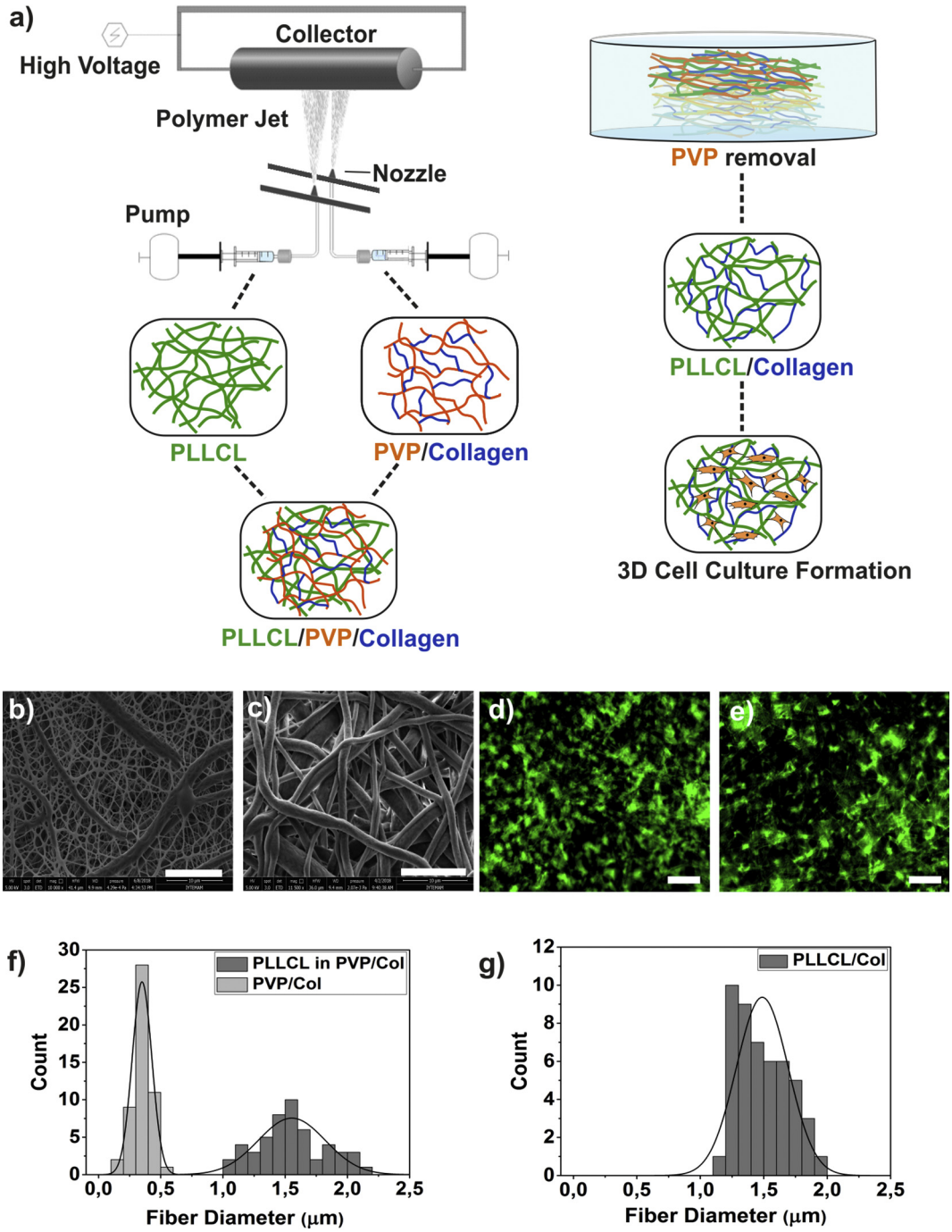

Fig. 1. a) Schematic illustration of biomimetic hybrid scaffold fabrication; including co-electrospinning process and polymer sacrificing agent removal. SEM micrographs of co-electrospun scaffolds; b) PLLCL/PVP/Col, c) PLLCL/Col (after PVP removal) (scale bar 10 μm). Immunostained scaffolds against Col Type I; d) PLLCL/PVP/Col, and e) PLLCL/Col (after PVP removal) (scale bar 20 μm). Fiber diameter distribution of f) PLLCL/PVP/Col and g) PLLCL/Col (after PVP removal) scaffolds.

Equal amount of CytoCalcein and PI is mixed in buffer solution and applied over samples with equal amount of culture media. After 30 min incubation at 37 °C, cells were analyzed using fluorescence microscope (Zeiss Observer Z1).

For SEM analysis 2500 cell/well were seeded on PLLCL/0.4%Col scaffolds. Prior to completion of incubation at 1, 3, 5 and 7 day, 4% paraformaldehyde was used to fix cells. Then, paraformaldehyde solution was washed three times with 1× PBS and scaffolds were dried at room temperature for further SEM analysis.

3. Result and discussion

3.1. Morphology of electrospun scaffolds

Electrospinning technique is utilized in this work to mimic fibrillar structure of native ECM. Optimization of electrospinning parameters was accomplished to obtain uniform homogeneous fibers, which is significant for 3D cell culture studies.

In recent studies, both collagen and hybrid polymers were commonly solubilized in HFIP which is highly toxic solvent, especially for biological applications. It was also reported that HFIP solubilized electrospun collagen gets mostly denaturated and lost its triple helix structure [42]. To avoid this, co-electrospinning of collagen was accomplished in the presence of water solubilized sacrificing polymers such as PVP.

First, to optimize the electrospinning parameters of PLLCL, varied concentrations of PLLCL (5%, 8% and 10%) were solubilized in 4.5:0.5 mL DCM:DMF solution [53,54]. At each concentration flow rate (3 mL/h) was constant, applied voltage and distance was varying in between 22–25 kV and 16–18 cm respectively. Elongated beads turned into uniform smooth homogeneous fibers and fiber diameters were increased with an increasing PLLCL concentration; 5% PLLCL 0.395 ± 0.99 μm, 8% PLLCL 0.522 ± 0.92 μm and 10% PLLCL was 1.312 ± 0.22 μm (Fig. SI1).

Later, to solubilize and facilitate the co-electrospinning of collagen, PVP was solubilized in water that was acidified with 0.1 M acetic acid solution. Co-electrospinning process was carried out with simultaneous deposition of PLLCL and PVP/Col solutions (Fig. 1a). The resulting PLLCL/PVP/Col scaffold showed distinct fiber morphologies based on utilized polymers; where thick fibers correspond to PLLCL, and thin fibers corresponds to PVP/Col (Fig. 1b and c). As demonstrated in SEM images, co-electrospun scaffolds exhibit bead-free, smooth fibers with interconnected porous structure. To solubilize and remove the polymer-sacrificing agent PVP, PLLCL/PVP/Col scaffold was washed with deionized water. After solubilization of sacrificing polymer only homogeneous, uniform and thick PLLCL/Col fibers remained confirming the removal of PVP (Fig. 1c). Also, fiber diameter distribution confirmed the presence and absence of PVP in both scaffolds; where Fig. 1b and c corresponds to Fig. 1f and g, respectively. The average fiber diameter of PLLCL in hybrid scaffold is 1.55 ± 0.27 μm and PVP fiber diameter is 0.349 ± 0.07 μm. After removal of polymer-sacrificing agent PVP, the average fiber diameter of PLLCL/Col scaffold is calculated as 1.50 ± 0.21 μm, confirming removal of PVP fibers.

3.2. Characterization of hybrid scaffold content

Immunostaining was performed to identify collagen in co-electrospun hybrid scaffolds both in the presence and absence of polymer sacrificing agent. FITC conjugated monoclonal IgG1 antibody against collagen type I was used to stain collagen on PLLCL/PVP/Col and PLLCL/Col scaffolds. Immunostaining analysis revealed relatively uniform distribution of collagen through PLLCL/PVP/Col and PLLCL/Col scaffolds (Fig. 1d and e). Even after removal of polymer sacrificing agent, strong fluorescence signal is obtained indicating the presence of collagen (Fig. 1e). As expected, no fluorescence signal was obtained for control group scaffolds; PLLCL and PLLCL/PVP (Fig. SI2).

On the other hand, removal of sacrificing agent PVP was confirmed by FTIR analysis (Fig. SI3). The PVP containing scaffold shows —OH stretching at 3434 cm^{-1}, C—N stretching of N-vinylpyrrolidone ring at 1283 cm^{-1} and C═O group at 1650 cm^{-1} representing amide groups. According to FTIR results PVP successfully removed from the hybrid scaffold by washing processes and only PLLCL/Col remained.

3.3. Mechanical characterization via tensile testing

Fig. 2b summarizes the tensile testing results of electrospun fibers and co-electrospun hybrid scaffold. The tensile modulus of pristine PLLCL was found to be 1.15 ± 0.02 MPa, however it increased to 6.32 ± 2.62 MPa by co-spinning, representing PLLCL/PVP. The increase in tensile modulus can be attributed to the inhomogeneous distribution of fiber diameters in PLLCL/PVP (see SEM images and fiber diameter distribution). Here, PVP fibers cause significant separation of PLLCL fibers, avoiding them to form large diameter fiber bundles. Hence, tensile modulus of PLLCL/PVP co-electrospun fibers exhibit substantial increase compared to pristine PLLCL fibers. In the case of formation of hybrid PLLCL/PVP/Col scaffold, the tensile modulus (1.01 ± 0.07 MPa) was found to be converging to the pristine PLLCL fibers and it increased to 1.84 ± 0.16 MPa upon removal of PVP sacrificing agent. The electrospinning process providing to fabricate close interacted chains because of the conformance of fibers in contrast to bulk polymer, and therefore it is expected to increase the strength while tension applied where fibers oriented to the same direction. Since PVP fibers were thinner than PLLCL, exhibiting weak mechanical properties by lowering the overall ultimate strength. However, by addition of collagen to scaffold the highest ultimate strength was obtained due to collagen's intramolecular hydrogen bonding properties inducing bundle formation by reinforcing PLLCL fibers. As seen in Fig. 2a the hybrid scaffold has exhibited higher tensile strength at all elongation state, which corresponds to the reinforcing effect of collagen to the PLLCL fibers. In overall, the reinforcing effect of collagen has proven by the substantial development in the mechanical property of the biomimetic hybrid scaffold.

a)

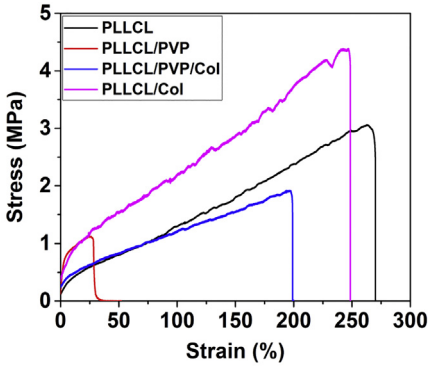

b)

Type of Scaffold	Tensile Modulus, MPa	Ultimate Tensile Stenght, MPa	Elongation at Break, %
PLLCL	1.15±0.02	2.90±0.34	262±15.9
PLLCL/PVP	6.32±2.62	1.13±0.01	25±5.8
PLLCL/PVP/Col	1.01±0.07	1.84±0.27	202±12.1
PLLCL/Col	1.84±0.16	4.27±0.16	245±7.3

Fig. 2. a) Stress-strain curve, and b) tensile test results of pristine PLLCL, PLLCL/PVP, PLLCL/PVP/Col and PLLCL/Col scaffolds.

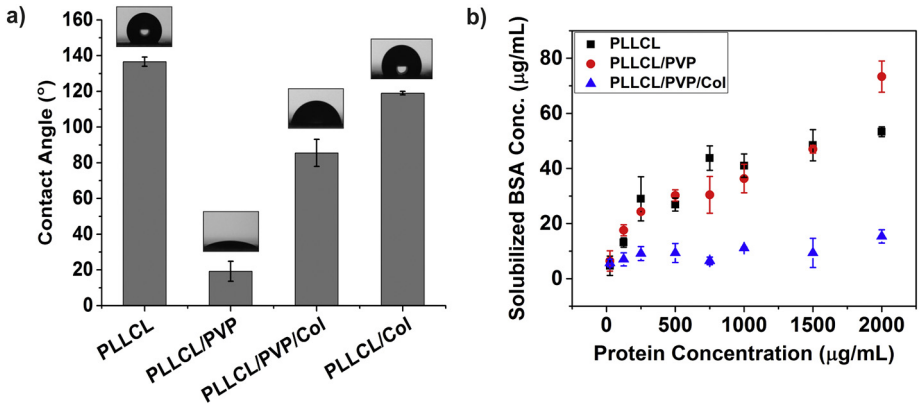

Fig. 3. a) Contact angle and b) protein adsorption results of pristine PLLCL, PLLCL/PVP, PLLCL/PVP/Col and PLLCL/Col scaffolds.

3.4. Contact angle analysis

Surface wettability has a direct impact on cell adhesion, growth, proliferation and differentiation [31,55]. Here surface wettability was examined in terms of contact angle analysis. Water contact angles were measured for pristine PLLCL, PLLCL/PVP, and PLLCL/Col scaffolds before and after removal of sacrificing agent, as shown in Fig. 3a. An average contact angle for pristine PLLCL was 136.6° ± 2.6 which indicates its hydrophobic nature. Average contact angle of PLLCL was reduced to 19.2° ± 5.6 after co-electrospinning with PVP due to highly hydrophilic property of PVP. After removal of sacrificing agent, contact angle value of PLLCL/Col scaffold increased to 119° ± 1.01° confirming the removal of hydrophilic PVP. Overall analysis showed that surface wettability can be adjusted based on collagen amount, and the co-electrospun scaffolds can be easily transformed in between hydrophilic and hydrophobic states.

3.5. Protein adsorption

For the success of a 3D cell culture approach, cell adhesion onto scaffold is crucial. Cell adhesion and proliferation occurs through favored cell-scaffold interaction, which is mostly triggered by cell receptors and ECM proteins. Therefore, protein adsorption on a scaffold is directly correlated with cell adhesion process. Here, protein adsorption analysis was done to investigate suitability of co-electrospun hybrid scaffolds for 3D cell culture applications. Firstly, scaffolds immersed in a range of BSA solutions (25–2000 μg/mL) and were incubated, and then adsorbed proteins were extracted from scaffolds by SDS detergent solubilization (Fig. 3b). Amount of adsorbed protein showed a steady increase and reached to an equilibrium at varied protein concentrations, which refers to the maximum protein holding capacity for each scaffold. Results confirmed that all scaffolds are favoring protein adsorption therefore expected to favor cell adhesion as well.

3.6. Biodegradation analysis

To determine the feasibility of using co-electrospun PLLCL/Col scaffold for regenerative purposes, biodegradation profile was evaluated by means of structural integrity, weight loss and porosity. Here, electrospun pristine PLLCL was utilized as a control scaffold (Fig. SI4). Fig. 4 shows biodegradation profile of PLLCL/Col scaffold during

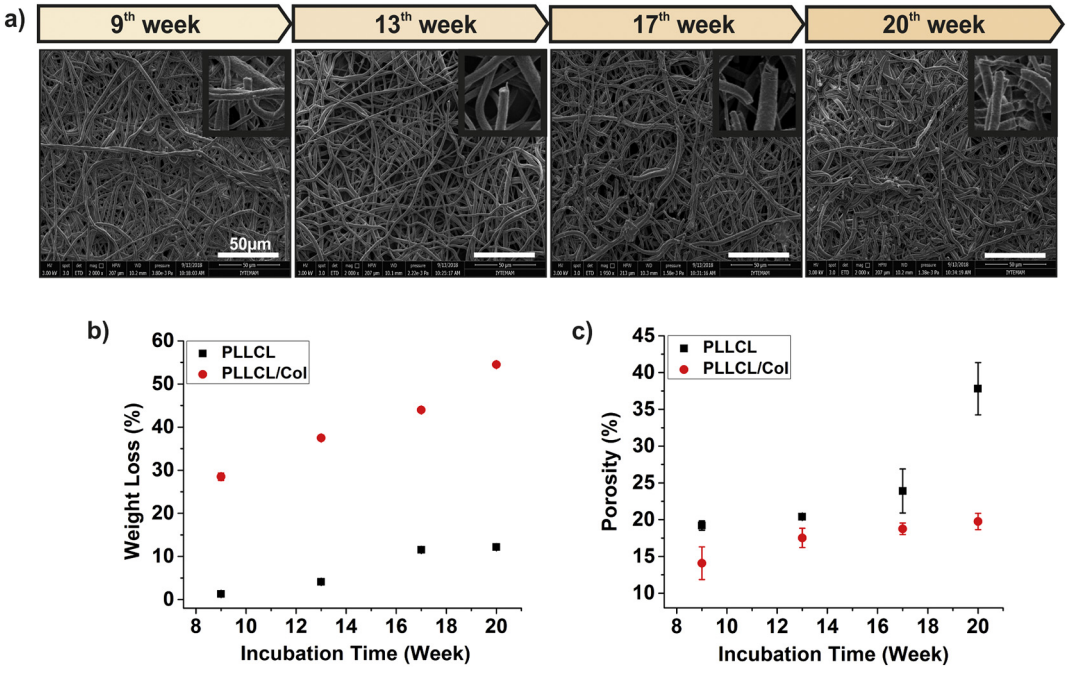

Fig. 4. a) SEM micrographs of enzymatic degradation of PLLCL/Col scaffold for 20 week incubation period, b) weight loss and c) porosity change profiles of pristine PLLCL and PLLCL/Col scaffolds during 20 week incubation.

20 weeks. As depicted in Fig. 4a, surface erosion and fiber cleavage occur starting from 9th week that confirms biodegradation and loss of structural integrity. During enzymatic degradation, the amount of weight loss increased from 1.3% ± 0.59 to 12.1% ± 0.47 for pristine PLLCL where it increased from 28.5% ± 0.85 to 54.5% ± 0.58 for PLLCL/Col scaffold in between 9th to 20th weeks (Fig. 4b). It was also observed that porosity increased up to 37.8% ± 3.5 for pristine PLLCL where it increased up to 19.8% ± 1.1 for PLLCL/Col at 20th week (Fig. 4c). Compared to pristine PLLCL, PLLCL/Col scaffold showed higher weight loss indicating higher degradation rate. Collagen is an amorphous biopolymer; therefore, it increases the degradation rate of hybrid scaffold.

3.7. Cell viability and toxicity of NIH 3T3 on PLLCL/Col hybrid scaffolds

In tissue engineering and 3D cell culture studies the ideal scaffold is expected to promote cell growth and differentiation. To evaluate the cell adhesion, spreading and proliferation, NIH 3T3 mouse fibroblast cells were seeded and cultured on PLLCL/Col hybrid scaffold. For comparison

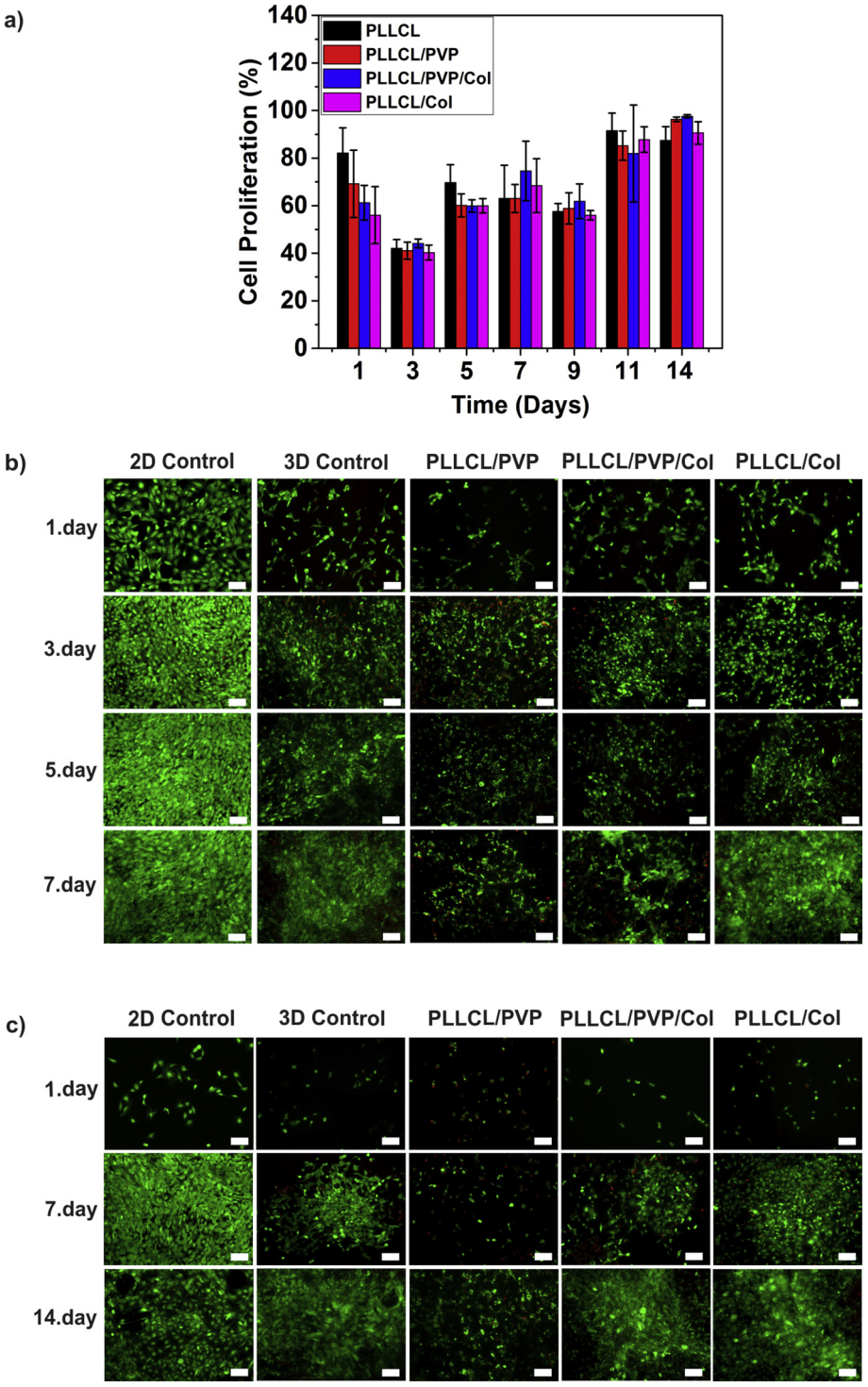

Fig. 5. a) Cell proliferation profiles of NIH 3T3 mouse fibroblast cells on biomimetic hybrid scaffolds, evaluated by Alamar blue assay. Cell viability evaluation of NIH 3T3 mouse fibroblast cells on biomimetic hybrid scaffolds for b) 1., 3., 5. and 7. day and c) 1., 7. and 14. day cell culture periods (scale bar: 100 μm). TCPS represents 2D Control and pristine PLLCL represents 3D Control. (Green: live cells, red: dead cells).

purposes pristine PLLCL was used as a 3D control scaffold and TCPS (tissue culture polystyrene) was utilized as a 2D control. The proliferation profile of NIH 3T3 cells on PLLCL/Col hybrid scaffolds are shown in Fig. 5a. Although the proliferation rate of NIH 3T3 cells were higher on PLLCL scaffold than that of cells on hybrid PLLCL/Col, NIH 3T3 cells were successfully proliferated on hybrid PLLCL/Col. Furthermore, cell viability and proliferation are investigated by live/dead analysis (Fig. 5b and c).

Cell proliferation is also affected by the removal of sacrificing agent PVP; on day 3 the number of adhered cells was slightly higher on PLLCL/Col scaffold than PLLCL/PVP/Col scaffold, indicating biocompatibility of hybrid PLLCL/Col scaffold. Proliferation and cell viability are increased on PVP removed scaffolds; preventing toxic effect of PVP and introducing biological functional groups of collagen probably provides improved microenvironment for cells. In 14-day cell culture studies, it was noted that the cell viability is decreasing for 2D control group due to excess proliferation, however 3D structure of hybrid PLLCL/Col scaffold promotes cellular adhesion and proliferation even in long term.

3.8. Cell morphology of NIH 3T3 cells on hybrid PLLCL/Col scaffolds

Cell-scaffold interaction and cell morphology was investigated for 7 days and analyzed by SEM as shown in Fig. 6a, b, c and d. After seeding and culturing of NIH 3T3 fibroblast cells on hybrid PLLCL/Col scaffold, cells started to adhere and spread over the fibers starting from day 1. Following 3 days in vitro cell culture, cells strongly adhered and easily spread on PLLCL/Col surface confirming that PLLCL/Col scaffold highly favors cell affinity while mimicking natural ECM microenvironment. Favored cell-scaffold interaction, as well filopodia formation (Fig. 6e) was observed which was likely due to collagen content that promotes cell adhesion. Later by day 7, PLLCL/Col scaffold was completely covered with thick layer of cell-sheets indicating that PLLCL/Col scaffold has good biocompatibility for 3D cell culture and tissue engineering applications.

4. Conclusion

In the field of scaffold-based tissue engineering natural biopolymers or hybrid scaffolds are commonly preferred over synthetic ones. Collagen is one of the mostly used and heavily investigated biopolymers, since it is the most abundant protein in human body and also a major component of native ECM. Electrospinning of collagen received great attention, since it mimics native ECM microenvironment while providing fibrillar structure and biocompatibility at the same time. However, harmful and toxic solvents such as; HFIP are mostly used to solubilize collagen. In the present study, a “toxic solvent free” methodology was

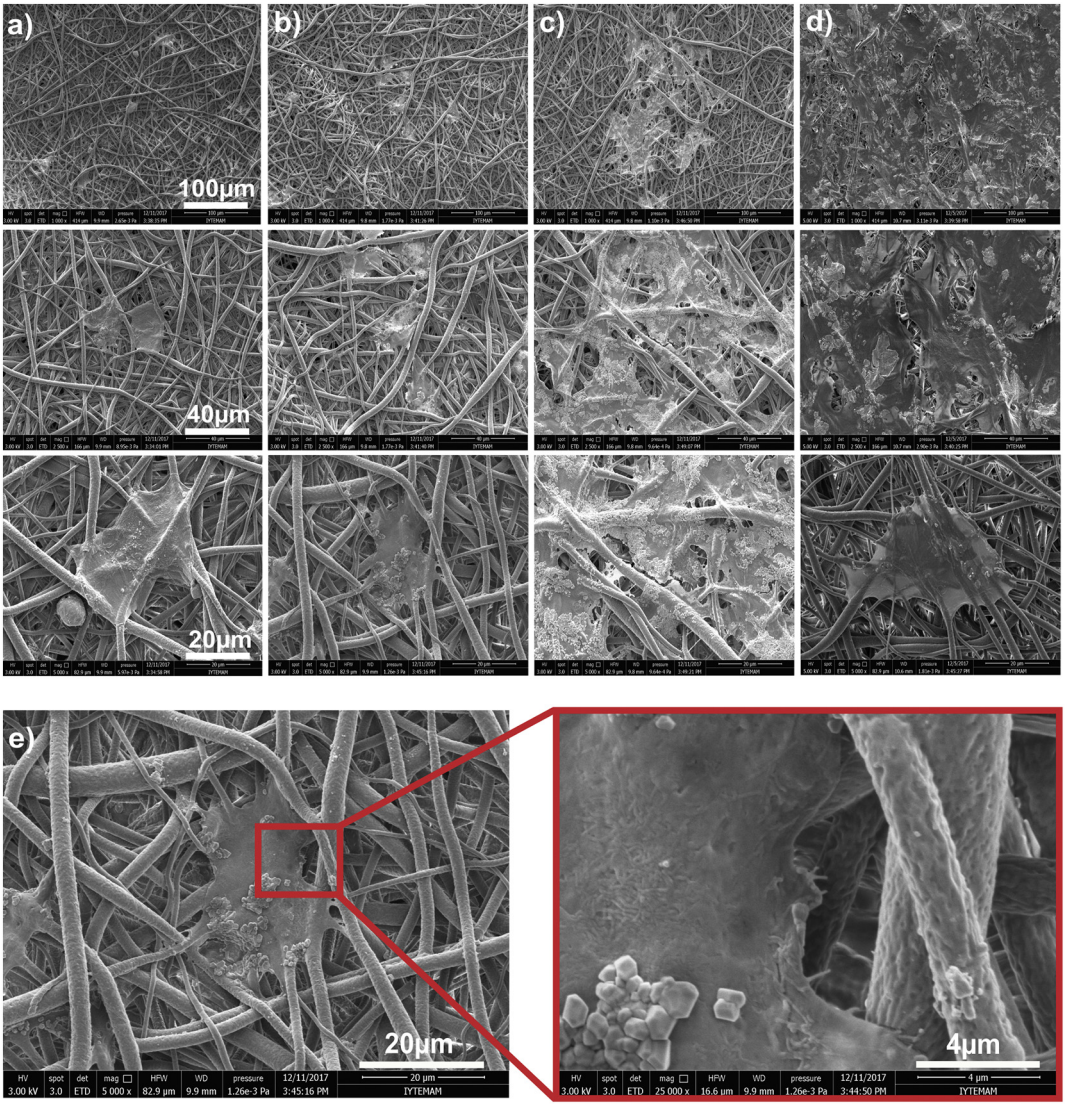

Fig. 6. SEM micrographs for evaluation of NIH 3T3 fibroblast cell adhesion and proliferation on PLLCL/Col scaffold a) 1, b) 3, c) 5 and d) 7. day cell culture periods. e) SEM micrograph showing filopodia formation of NIH 3T3 fibroblast cells on PLLCL/Col scaffold.

developed to avoid heavy chemicals. Instead of toxic solvents, water-based sacrificing polymer PVP was utilized for co-electrospinning process; later it was easily removed through rinsing with water. A biomimetic hybrid scaffold, PLLCL/Col, that mimics the native structure and microenvironment of ECM, has been fabricated combining sacrificing agent approach with co-electrospinning process. PLLCL/Col scaffold exhibits ECM-like 3D network structure, while addition of collagen improved mechanical and surface properties of scaffold for biological applications. Moreover, presence of collagen improved cell adhesion and proliferation on long-term cultures compared to standard 2D cell culture models. It has been demonstrated that developed methodology is a novel and bio-friendly method that is especially suitable for 3D cell culture and tissue engineering applications.

Declaration of competing interest

The authors declare no competing financial interest.

Acknowledgements

This study was supported by IYTE BAP grant (2016IYTE70). The authors acknowledge İzmir Institute of Technology Biotechnology and Bioengineering Research and Application Center, and İzmir Institute of Technology Materials Research Center for the instrumental facilities provided to accomplish this study.

Appendix A. Supplementary data

Supplementary data to this article can be found online at https://doi.org/10.1016/j.ijbiomac.2019.08.082.

References

[1] A. Ovsianikov, V. Mironov, J. Stampf, R. Liska, Engineering 3D cell-culture matrices: multiphoton processing technologies for biological and tissue engineering applications, Expert Rev. Med. Devices 9 (6) (2012) 613–633.
[2] L.G. Griffith, M.A. Swartz, Capturing complex 3D tissue physiology in vitro, Nat. Rev. Mol. Cell Biol. 7 (3) (2006) 211.
[3] G.D. Prestwich, Simplifying the extracellular matrix for 3-D cell culture and tissue engineering: a pragmatic approach, J. Cell. Biochem. 101 (6) (2007) 1370–1383.
[4] K. Duval, H. Grover, L.H. Han, Y. Mou, A.F. Pegoraro, J. Fredberg, Z. Chen, Modeling physiological events in 2D vs. 3D cell culture, Physiology (Bethesda) 32 (4) (2017) 266–277.
[5] J. Lee, M.J. Cuddihy, N.A. Kotov, Three-dimensional cell culture matrices: state of the art, Tissue Eng. Part B Rev. 14 (1) (2008) 61–86.
[6] W.L. Grayson, T.P. Martens, G.M. Eng, M. Radisic, G. Vunjak-Novakovic, Biomimetic approach to tissue engineering, Semin. Cell Dev. Biol. 20 (6) (2009) 665–673.
[7] J.B. Kim, Three-dimensional tissue culture models in cancer biology, Semin. Cancer Biol. (2005) 365–377 Elsevier.
[8] L.G. Griffith, G. Naughton, Tissue engineering—current challenges and expanding opportunities, Science 295 (5557) (2002) 1009–1014.
[9] A.G. Mikos, Y. Bao, L.G. Cima, D.E. Ingber, J.P. Vacanti, R. Langer, Preparation of poly (glycolic acid) bonded fiber structures for cell attachment and transplantation, J. Biomed. Mater. Res. A 27 (2) (1993) 183–189.
[10] A.G. Mikos, G. Sarakinos, S.M. Leite, J.P. Vacanti, R. Langer, Laminated three-dimensional biodegradable foams for use in tissue engineering, The Biomaterials: Silver Jubilee Compendium, vol. 14, 1993, pp. 93–100.
[11] A.G. Mikos, A.J. Thorsen, L.A. Czerwonka, Y. Bao, R. Langer, D.N. Winslow, J.P. Vacanti, Preparation and characterization of poly (L-lactic acid) foams, Polymer 35 (5) (1994) 1068–1077.
[12] A.G. Mikos, G. Sarakinos, J.P. Vacanti, R.S. Langer, L.G. Cima, Biocompatible polymer membranes and methods of preparation of three dimensional membrane structures, Google Patents, 1996.
[13] C.X.F. Lam, X. Mo, S.-H. Teoh, D. Hutmacher, Scaffold development using 3D printing with a starch-based polymer, Mater. Sci. Eng. C 20 (1–2) (2002) 49–56.
[14] A. Arslan-Yildiz, R. El Assal, P. Chen, S. Guven, F. Inci, U. Demirci, Towards artificial tissue models: past, present, and future of 3D bioprinting, Biofabrication 8 (1) (2016), 014103.
[15] D. Karalekas, Study of the mechanical properties of nonwoven fibre mat reinforced photopolymers used in rapid prototyping, Mater. Des. 24 (8) (2003) 665–670.
[16] F. Wiria, K. Leong, C. Chua, Y. Liu, Poly-ε-caprolactone/hydroxyapatite for tissue engineering scaffold fabrication via selective laser sintering, Acta Biomater. 3 (1) (2007) 1–12.
[17] D.W. Hutmacher, T. Schantz, I. Zein, K.W. Ng, S.H. Teoh, K.C. Tan, Mechanical properties and cell cultural response of polycaprolactone scaffolds designed and fabricated via fused deposition modeling, J. Biomed. Mater. Res. A 55 (2) (2001) 203–216.
[18] S. Deville, E. Saiz, A.P. Tomsia, Freeze casting of hydroxyapatite scaffolds for bone tissue engineering, Biomaterials 27 (32) (2006) 5480–5489.
[19] H.-W. Kang, Y. Tabata, Y. Ikada, Fabrication of porous gelatin scaffolds for tissue engineering, Biomaterials 20 (14) (1999) 1339–1344.
[20] C.M. Murphy, M.G. Haugh, F.J. O'Brien, The effect of mean pore size on cell attachment, proliferation and migration in collagen–glycosaminoglycan scaffolds for bone tissue engineering, Biomaterials 31 (3) (2010) 461–466.
[21] R.A. Quirk, R.M. France, K.M. Shakesheff, S.M. Howdle, Supercritical fluid technologies and tissue engineering scaffolds, Curr. Opinion Solid State Mater. Sci. 8 (3–4) (2004) 313–321.
[22] A. Zellander, R. Gemeinhart, A. Djalilian, M. Makhsous, S. Sun, M. Cho, Designing a gas foamed scaffold for keratoprosthesis, Mater. Sci. Eng. C 33 (6) (2013) 3396–3403.
[23] H. Haugen, V. Ried, M. Brunner, J. Will, E. Wintermantel, Water as foaming agent for open cell polyurethane structures, J. Mater. Sci. Mater. Med. 15 (4) (2004) 343–346.
[24] C.R. Wittmer, X. Hu, P.C. Gauthier, S. Weisman, D.L. Kaplan, T.D. Sutherland, Production, structure and in vitro degradation of electrospun honeybee silk nanofibers, Acta Biomater. 7 (10) (2011) 3789–3795.
[25] Z.-M. Huang, Y.-Z. Zhang, M. Kotaki, S. Ramakrishna, A review on polymer nanofibers by electrospinning and their applications in nanocomposites, Compos. Sci. Technol. 63 (15) (2003) 2223–2253.
[26] M.S. Kim, G. Kim, Three-dimensional electrospun polycaprolactone (PCL)/alginate hybrid composite scaffolds, Carbohydr. Polym. 114 (2014) 213–221.
[27] R. Inai, M. Kotaki, S. Ramakrishna, Structure and properties of electrospun PLLA single nanofibres, Nanotechnology 16 (2) (2005) 208–213.
[28] A. Edwards, D. Jarvis, T. Hopkins, S. Pixley, N. Bhattarai, Poly(epsilon-caprolactone)/keratin-based composite nanofibers for biomedical applications, J Biomed Mater Res B Appl Biomater 103 (1) (2015) 21–30.
[29] X. He, L. Cheng, X. Zhang, Q. Xiao, W. Zhang, C. Lu, Tissue engineering scaffolds electrospun from cotton cellulose, Carbohydr. Polym. 115 (2015) 485–493.
[30] T. Jiang, E.J. Carbone, K.W.H. Lo, C.T. Laurencin, Electrospinning of polymer nanofibers for tissue regeneration, Prog. Polym. Sci. 46 (2015) 1–24.
[31] X. He, W. Fu, B. Feng, H. Wang, Z. Liu, M. Yin, W. Wang, J. Zheng, Electrospun collagen–poly (L-lactic acid-co-ε-caprolactone) membranes for cartilage tissue engineering, Regen. Med. 8 (4) (2013) 425–436.
[32] G.E. Wnek, M.E. Carr, D.G. Simpson, G.L. Bowlin, Electrospinning of nanofiber fibrinogen structures, Nano Lett. 3 (2) (2003) 213–216.
[33] E.K. Brenner, J.D. Schiffman, E.A. Thompson, L.J. Toth, C.L. Schauer, Electrospinning of hyaluronic acid nanofibers from aqueous ammonium solutions, Carbohydr. Polym. 87 (1) (2012) 926–929.
[34] J. Rnjak-Kovacina, S.G. Wise, Z. Li, P.K. Maitz, C.J. Young, Y. Wang, A.S. Weiss, Electrospun synthetic human elastin:collagen composite scaffolds for dermal tissue engineering, Acta Biomater. 8 (10) (2012) 3714–3722.
[35] R.M. Aghdam, S. Najarian, S. Shakhesi, S. Khanlari, K. Shaabani, S. Sharifi, Investigating the effect of PGA on physical and mechanical properties of electrospun PCL/PGA blend nanofibers, J. Appl. Polym. Sci. 124 (1) (2012) 123–131.
[36] Y. Chen, D. Zeng, L. Ding, X.-L. Li, X.-T. Liu, W.-J. Li, T. Wei, S. Yan, J.-H. Xie, L. Wei, Three-dimensional poly-(ε-caprolactone) nanofibrous scaffolds directly promote the cardiomyocyte differentiation of murine-induced pluripotent stem cells through Wnt/β-catenin signaling, BMC Cell Biol. 16 (1) (2015) 22.
[37] K. Gelse, Collagens—structure, function, and biosynthesis, Adv. Drug Deliv. Rev. 55 (12) (2003) 1531–1546.
[38] M.K. Gordon, R.A. Hahn, Collagens, Cell Tissue Res. 339 (1) (2010) 247.
[39] A.D. Theocharis, S.S. Skandalis, C. Gialeli, N.K. Karamanos, Extracellular matrix structure, Adv. Drug Deliv. Rev. 97 (2016) 4–27.
[40] R. Maynes, Structure and Function of Collagen Types, Elsevier, 2012.
[41] Z. Chen, P. Wang, B. Wei, X. Mo, F. Cui, Electrospun collagen–chitosan nanofiber: a biomimetic extracellular matrix for endothelial cell and smooth muscle cell, Acta Biomater. 6 (2) (2010) 372–382.
[42] S.H. Park, T.G. Kim, H.C. Kim, D.Y. Yang, T.G. Park, Development of dual scale scaffolds via direct polymer melt deposition and electrospinning for applications in tissue regeneration, Acta Biomater. 4 (5) (2008) 1198–1207.
[43] J.A. Matthews, G.E. Wnek, D.G. Simpson, G.L. Bowlin, Electrospinning of collagen nanofibers, Biomacromolecules 3 (2) (2002) 232–238.
[44] Y. Xu, J. Wu, H. Wang, H. Li, N. Di, L. Song, S. Li, D. Li, Y. Xiang, W. Liu, X. Mo, Q. Zhou, Fabrication of electrospun poly(L-lactide-co-epsilon-caprolactone)/collagen nanoyarn network as a novel, three-dimensional, macroporous, aligned scaffold for tendon tissue engineering, Tissue Eng. Part C Methods 19 (12) (2013) 925–936.
[45] I.K. Kwon, T. Matsuda, Co-electrospun nanofiber fabrics of poly (L-lactide-co-ε-caprolactone) with type I collagen or heparin, Biomacromolecules 6 (4) (2005) 2096–2105.
[46] A. Yin, K. Zhang, M.J. McClure, C. Huang, J. Wu, J. Fang, X. Mo, G.L. Bowlin, S.S. Al-Deyab, M. El-Newehy, Electrospinning collagen/chitosan/poly (L-lactic acid-co-ε-caprolactone) to form a vascular graft: mechanical and biological characterization, J. Biomed. Mater. Res. A 101 (5) (2013) 1292–1301.
[47] J. Xie, M. Ihara, Y. Jung, I.K. Kwon, S.H. Kim, Y.H. Kim, T. Matsuda, Mechano-active scaffold design based on microporous poly (L-lactide-co-ε-caprolactone) for articular cartilage tissue engineering: dependence of porosity on compression force-applied mechanical behaviors, Tissue Eng. 12 (3) (2006) 449–458.
[48] S.H. Bhang, S.I. Jeong, T.J. Lee, I. Jun, Y.B. Lee, B.S. Kim, H. Shin, Electroactive electrospun polyaniline/poly [(L-lactide)-co-(ε-caprolactone)] fibers for control of neural cell function, Macromol. Biosci. 12 (3) (2012) 402–411.

[49] S.I. Jeong, S.H. Kim, Y.H. Kim, Y. Jung, J.H. Kwon, B.-S. Kim, Y.M. Lee, Manufacture of elastic biodegradable PLCL scaffolds for mechano-active vascular tissue engineering, J. Biomater. Sci. Polym. Ed. 15 (5) (2004) 645–660.
[50] X.M. Mo, C.Y. Xu, M. Kotaki, S. Ramakrishna, Electrospun P(LLA-CL) nanofiber: a biomimetic extracellular matrix for smooth muscle cell and endothelial cell proliferation, Biomaterials 25 (10) (2004) 1883–1890.
[51] C. Vaquette, C. Frochot, R. Rahouadj, S. Muller, X. Wang, Mechanical and biological characterization of a porous poly-L-lactic acid-co-ϵ-caprolactone scaffold for tissue engineering, Soft Mater. 6 (1) (2008) 25–33.
[52] C.P. Laurent, C. Vaquette, X. Liu, J.F. Schmitt, R. Rahouadj, Suitability of a PLCL fibrous scaffold for soft tissue engineering applications: a combined biological and mechanical characterisation, J. Biomater. Appl. 32 (9) (2018) 1276–1288.
[53] L. Du, H. Xu, Y. Zhang, F. Zou, Electrospinning of polycaprolatone nanofibers with DMF additive: the effect of solution proprieties on jet perturbation and fiber morphologies, Fiber Polym. 17 (5) (2016) 751–759.
[54] R. Machado, A. Da Costa, D.M. Silva, A.C. Gomes, M. Casal, V. Sencadas, Antibacterial and antifungal activity of poly (lactic acid)–bovine Lactoferrin nanofiber membranes, Macromol. Biosci. 18 (3) (2018), 1700324.
[55] K. Zhang, H. Wang, C. Huang, Y. Su, X. Mo, Y. Ikada, Fabrication of silk fibroin blended P(LLA-CL) nanofibrous scaffolds for tissue engineering, J. Biomed. Mater. Res. A 93 (3) (2010) 984–993.